ASSESSMENT OF RF SYSTEM CAPABILITY IN THE J-PARC MAIN RING TOWARD 1.3 MW OPERATION

K. Seiya*, K. Adachi, K. Hara,, K. Hasegawa, C. Ohmori, H. Okita,
T. Shimada, Y. Sugiyama, F. Tamura, M. Yamamoto, M. Yoshii
Japan Proton Accelerator Research Complex, Tōkai Mura, Japan

Abstract

The J-PARC Main Ring plans to increase its beam power from 830 kW to 1.3 MW for the Hyper-Kamiokande neutrino experiment by 2028. To enable this high-power operation, the RF system has been upgraded by increasing both the number of RF cavities and the anode current of the tetrode amplifiers. However, the required anode current is approaching the operational limits of the RF tubes, and several associated power-supply systems are also close to their design limits.

Traditionally, the anode current has been estimated using a phasor diagram model. In this study, we instead evaluate the anode current using LTspice simulations, which allow detailed modeling of the vacuum tubes, cavity impedance, and beam loading. An LTspice model of the Main Ring RF system has been developed, including a magnetic-alloy-loaded cavity, two 600 kW tetrode tubes, and an eight bunch beam with a total intensity of 3.3×10^{14} protons per pulse. This model enables estimation of anode and screen grid currents, and the results are compared with measurements.

This paper presents LTspice-based RF system calculations for the Main Ring and evaluates the RF power requirements for 1.3 MW beam operation.

INTRODUCTION

The J-PARC Main Ring plans to increase its beam power from 830 kW to 1.3 MW for the Hyper-Kamiokande neutrino experiment by 2028 [1]. To enable this higher power operation, the RF system has been upgraded by increasing both the number of cavities and the anode current of the tetrode tubes. However, the required anode current is now approaching the maximum capability of the tubes, and several associated power supply systems are also nearing their operational limits [2].

Traditionally, the anode current has been estimated using a phasor diagram approach [3–5]. As an alternative, we evaluate the current using LTspice simulations, which can incorporate the vacuum tube characteristics, cavity impedance, and beam loading [6, 7]. We have constructed an LTspice model of the Main Ring RF system that includes the impedance of the magnetic alloy loaded RF cavity, two 600 kW tetrode tubes, and the beam current corresponding to eight bunches with a total intensity of 3.3×10^{14} protons. This allows us to estimate not only the anode current but also the screen grid currents, and the simulation results have been compared with measurements.

* kiyomis@post.kek.jp

In this paper, we present LTspice-based RF system calculations for the Main Ring and evaluate the RF power requirements necessary to achieve 1.3 MW beam operation.

MR RF SYSTEM AND OPERATION

Eight bunches are injected from the Rapid Cycling Synchrotron (RCS) and accelerated while the RF frequency is ramped from 1.67 MHz to 1.72 MHz. The total injection voltage is 160 kV, which is increased linearly to 450 kV after completion of injection. Since the harmonic number is 9, the beam consists of a train of eight filled buckets and one empty bucket.

Figure 1 (left) shows a typical wall current monitor (WCM) signal at extraction energy, measured using a 2 GHz sampling oscilloscope over 5 μs. The signal is extended to the revolution frequency by repeating the recorded waveform.

To provide 450 kV, nine RF cavities are used at the fundamental frequency. Each cavity consists of three or four cells, each containing a ceramic gap and magnetic alloy cores. A single final amplifier feeds multiple gaps in parallel, resulting in a gap voltage of 13.45 kV and a total of 33 accelerating gaps.

The shunt impedance of the four-gap cavity is approximately 400 Ω, with a quality factor of about 21.

Figure 1 (right) shows the FFT spectrum of the WCM signal at extraction, overlaid with the cavity impedance. The low-level RF (LLRF) system controls not only the fundamental harmonic $h = 9$ but also neighboring harmonics ($h = 6, 7, 8, 10, 11, 12$) to achieve the desired gap voltage using I/Q feedback [8].

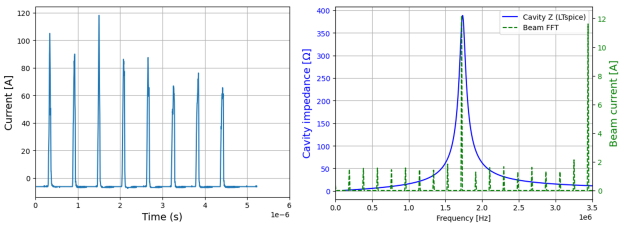

Figure 1: (left) WCM signal was extended to the revolution frequency by repeating the last oscilloscope data, (right) shows the FFT result of the WCM signal at extraction, overlaid with the cavity impedance.

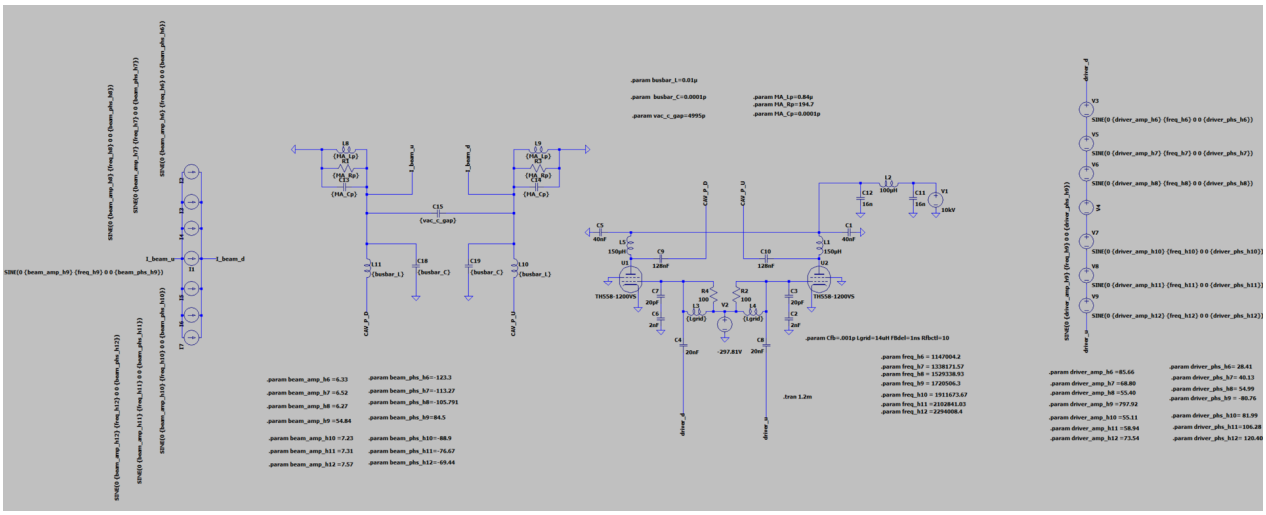

Figure 2: LTspice model with the cavity, final-stage amplifier, driver voltage source, and beam current source.

ANODE CURRENT ESTIMATION WITHOUT BEAM LOADING

RF System Modeling in LTspice

The RF system was modeled in LTspice, including the RF cavity, final-stage amplifier, driver voltage source, and beam current source, as shown in Fig. 2.

The four gap cavity was represented by two resonant circuits connected in series with a large coupling capacitor. In the actual system, the four cells are connected in parallel using busbars. Several vacuum capacitors are installed at each gap to reduce the resonant frequency to approximately 1.73 MHz and to increase the cavity quality factor to about 21. The total capacitance of the vacuum capacitors is approximately 5000 pF, while the capacitance of each accelerating gap is about 20 pF.

Two tetrode vacuum tubes (TH589E) are used in the final amplifier stage. During normal operation, the screen grid voltage is set to 1200 V, the control-grid voltage is approximately 300 V, and the plate voltage is 10 kV. The tubes are coupled to the accelerating gaps through DC blocking capacitors.

The RF system operates in class-AB push-pull mode, where the two amplifier outputs drive the cavity with opposite phases, resulting in opposite polarities across the accelerating gaps.

Both the driver voltage source and the beam current source include the fundamental RF component ($h = 9$) and six neighboring harmonics ($h = 6, 7, 8, 10, 11, 12$). Other frequency components are neglected in the present analysis.

Cavity Impedance Measurement in LTspice

The cavity impedance was measured using a network analyzer with and without the RF amplifier. Using AC analysis in LTspice, the impedance was obtained by applying a 1 V small signal excitation and sweeping the frequency from 100 kHz to 10 MHz, with the driver and beam sources disabled. Figure 3 compares the measured and simulated impedance. The left plot shows the magnitude of the impedance, and the right plot shows the phase response.

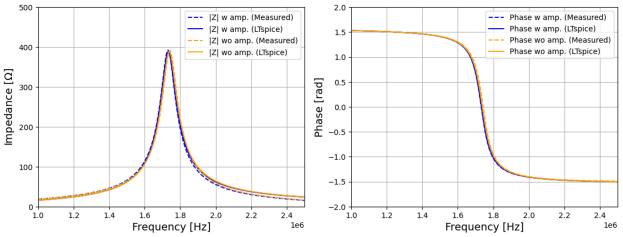

Figure 3: Comparison between measured and simulated cavity impedance. (left) Magnitude of impedance. (right) Phase response.

Gap Voltage and Anode Current Estimation

To obtain the gap voltage in LTspice, a transient analysis was performed for 1.2 ms to ensure that the signals had reached a steady state. The voltages were then analyzed using the last three revolution periods of the simulation data. The driver voltage was adjusted along the acceleration cycle from injection to extraction to reproduce the target cavity gap voltage at the fundamental frequency under beam-free conditions. Figure 4 shows the comparison between the target voltage and the LTspice simulation after tuning.

The anode current was then evaluated using the adjusted driver voltage. Figure 4 (right) compares the measured anode current for six four gap cavities (Cavities 3–8) with the LTspice results. The simulation reproduces the overall trend of the measurements; however, a systematic deviation of approximately 10 % is observed. The origin of this discrepancy is currently under investigation.

ANODE CURRENT ESTIMATION WITH BEAM LOADING

This section describes the LTspice-based procedure used to estimate the anode current under beam loading conditions, including harmonic components from $h = 6$ to $h = 12$. Transient analyses were performed for 1.2 ms in LTspice to

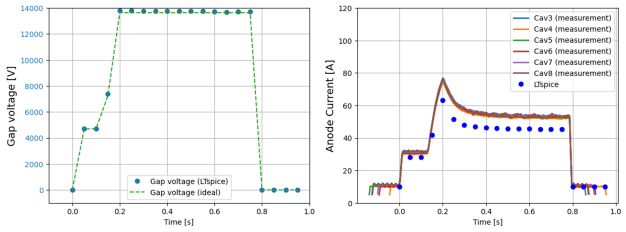

Figure 4: Comparison between measurements and LTspice simulation after voltage tuning. (left) Cavity gap voltage over the acceleration cycle. (right) Anode current for six four gap cavities (Cavities 3–8) compared with the LTspice results.

reach steady state, and the voltages were analyzed over the last three revolution periods.

Model Setup and Harmonic Beam Current Definition

The LTspice model includes the RF cavity, final stage amplifier, driver voltage source, and beam current source. The beam current waveform is reconstructed from the wall current monitor (WCM) signal and its FFT spectrum. The amplitude and phase of each harmonic component (h = 6–12) are extracted and used as inputs for the beam current source.

Transfer Function Identification

The cavity harmonic transfer function $H(h)$ is evaluated without beam loading. A small-signal excitation (V_{drive} = 100 V) is applied, and the resulting cavity response is used to obtain the complex transfer function under beam-free conditions.:

$$H(h) = \frac{V_h}{V_{\mathrm{drive}}} = \frac{V_h^{\mathrm{raw}} e^{-j\phi_{\mathrm{ref},h}}}{100},$$

where f_0 is the revolution frequency, f_h is the harmonic frequency, V_h^{raw} is the complex IQ-demodulated cavity voltage, and $\phi_{\mathrm{ref},h}$ is the local IQ reference phase.

Phase Adjustment and Synchronous Condition

The relative phase between the beam current and the cavity voltage is adjusted to satisfy the synchronous phase condition. The target cavity voltage defines the RF reference phase.

Beam-loaded Simulation and I/Q Feedback Procedure

Using the obtained transfer function $H(h)$, the beam-loaded operation is simulated including harmonic beam current components. The cavity voltage is represented in the complex I/Q plane and compared with the target voltage in the local reference frame. The voltage error is corrected using an inverse model of the cavity response.

A proportional feedback controller independently updates the in-phase (I) and quadrature (Q) components of the drive

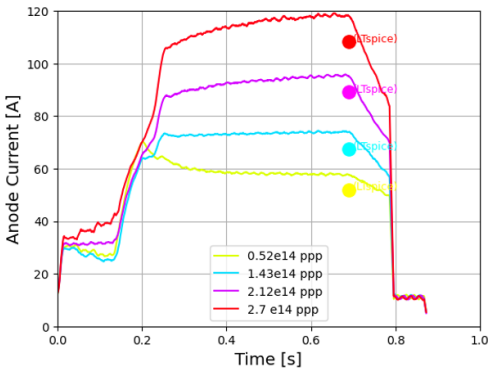

Figure 5: Comparison between the measured and simulated anode currents as a function of beam intensity, varied from 0.5×10^{14} ppp to 2.7×10^{14} ppp.

signal in an iterative manner:

$$I_h^{(n+1)} = I_h^{(n)} + K_p \,\mathrm{Re}\left(\frac{e_h}{H(h)}\right),$$

$$Q_h^{(n+1)} = Q_h^{(n)} + K_p \,\mathrm{Im}\left(\frac{e_h}{H(h)}\right),$$

$$D_h^{(n+1)} = I_h^{(n+1)} + jQ_h^{(n+1)},$$

where e_h is the complex voltage error for harmonic h, $H(h)$ is the measured harmonic transfer function, K_p is the proportional gain, and D_h is the complex drive vector.

Anode Current Measurements

The LTspice simulation was performed at t = 0.69 s, corresponding to a synchronous phase of 35°. This operating point is chosen just before the phase is reduced toward extraction, where the anode current reaches its maximum value.

Figure 5 compares the measured and simulated anode currents as a function of beam intensity, varied from 0.5×10^{14} ppp to 2.7×10^{14} ppp.

The simulation reproduces the overall dependence on beam intensity; however, the calculated anode current is systematically lower by approximately 10 % compared with measurements. This trend is consistent with beam-free comparison results. The remaining discrepancy is not yet fully understood and is under investigation.

SUMMARY

The J-PARC Main Ring RF system requires higher anode current to support the Hyper-K upgrade to 3.3×10^{14} protons per pulse and compensate for increased beam loading.

An LTspice model of the RF system was developed, including the cavity, tetrode amplifiers, driver source, and beam current harmonics from h = 6 to h = 12. The simulation reproduces the overall measured anode current behavior, although some discrepancies remain.

Future work will improve the cavity impedance and tetrode models, together with additional grid and gap voltage measurements for more detailed comparison with simulations.

REFERENCES

[1] S. Igarashi *et al.*, "Accelerator design for 1.3 MW beam power operation of the J-PARC Main Ring", *PTEP*, vol. 2021, no. 3, p. 033G01, 2021. doi:10.1093/pept/ptab011

[2] K. K. Seiya *et al.*, "RF system upgrade for 1.3 MW operation of J-PARC main ring", in *Proc. IPAC'24*, Nashville, TN, USA, May 2024, pp. 1017–1020. doi:10.18429/JACoW-IPAC2024-TUPC10

[3] Y. Sugiyama *et al.*, "Estimation of the anode power supply current of the J-PARC MR RF system for 1.36 s cycle operation", in *Proc. IPAC'23*, Venice, Italy, May 2023, pp. 2320–2322. doi:10.18429/JACoW-IPAC2023-TUPM056

[4] K. Seiya *et al.*, "RF Anode current estimation for high power operation at J-PARC Main Ring", in *J-PARC symposium proceedings*, to be published.

[5] K. Seiya *et al.*,"Estimation of the required current on the anode power supply for high power operation in the J-PARC Main Ring", in *Proc. IPAC'25*, Taipei, Taiwan, Jun. 2025, pp. 2443–2446. doi:10.18429/JACoW-IPAC2025-WEPS132

[6] F. Tamura *et al.*, "Simulations of Beam Loading Compensation in a Wideband Accelerating Cavity Using a Circuit Simulator Including a LLRF Feedback Control", Melbourne, Australia, May 2019, pp. 2863–2866. doi:10.18429/JACoW-IPAC2019-WEPRB026

[7] H. Okita *et al.*, "Circuit simulation model for the RF system of J-PARC RCS ", in *Proceedings of the 21st Annual Meeting of Particle Accelerator Society of Japan*, Yamagata, Japan, Aug. 2024, paper THP069, pp. 765–769.

[8] Y. Sugiyama *et al.*, "Next Generation LLRF Control System for J-PARC MR", in *Proc. the 19th Annual Meeting of PASJ*, Online, Japan, pp. 92–96, Oct. 2022.